Published for SISSA by Springer

Received: *July 26, 2011*
Revised: *January 28, 2012*
Accepted: *February 13, 2012*
Published: *February 24, 2012*

# Next-to-leading-order Monte Carlo simulation of diphoton production in hadronic collisions

**Luca D'Errico**[a,b] **and Peter Richardson**[b]

[a] *Institut für Theoretische Physik, University of Karlsruhe, KIT, 76128, Germany*
[b] *Institute of Particle Physics Phenomenology, Department of Physics, University of Durham, DH1 3LE, U.K.*

*E-mail:* derrico@particle.uni-karlsruhe.de, peter.richardson@durham.ac.uk

Abstract: We present a method, based on the positive weight next-to-leading-order matching formalism (POWHEG), to simulate photon production processes at next-to-leading-order (NLO). This technique is applied to the simulation of diphoton production in hadron-hadron collisions. The algorithm consistently combines the parton shower and NLO calculation, producing only positive weight events. The simulation includes both the photon fragmentation contribution and a full implementation of the truncated shower required to correctly describe soft emissions in an angular-ordered parton shower.

Keywords: QCD Phenomenology

ArXiv ePrint: 1106.3939



doi:10.1007/JHEP02(2012)130

## Contents





# 1 Introduction

The production of photons via perturbative processes is very important for both the search for the Higgs boson and other new physics, via photon pair production, and for the study of QCD and experimental effects, in particular the jet-energy scale, in the production of a photon in association with a jet. To study these processes in detail in hadron-hadron collisions we need an accurate Monte Carlo simulation. In this paper we present a new approach for the simulation of these processes and illustrate it with the simulation of photon pair production.

Monte Carlo event generators simulate events by combining fixed-order matrix elements, parton showers and hadronization models. The first programs used leading-order (LO) matrix elements, together with the parton shower approximation which describes soft and collinear emission. Recently different approaches correcting the emission of high transverse momentum, $p_T$, partons have been introduced.[1]

Different algorithms have been developed to provide a better description of the hardest emission, including the full next-to-leading-order cross section. In the approach of Frixione and Webber (MC@NLO) [31, 32], the parton shower approximation is subtracted from the real emission contribution to the next-to-leading-order cross section and combined with the virtual correction. This method was successfully applied to many different processes [33–40]. However, this approach has two drawbacks: it generates weights that are not positive definite and its implementation depend s on the parton shower algorithm.

[1] See ref. [1] for a recent review of the older techniques [2–19] and techniques for improving the simulation of multiple hard QCD radiation [20–30].

These drawbacks have been addressed with a new method introduced by Nason [41, 42], the POsitive Weight Hardest Emission Generator (POWHEG) approach. This method generates positive weights and is implemented in a way that does not depend on the details of the parton shower algorithm. Nevertheless, the parton shower algorithm must have a well defined structure: a *truncated shower* simulating wide angle soft emission; followed by the emission with highest transverse momentum ($p_T$); followed by a *vetoed shower* simulating softer radiation. The hardest emission is generated by a Sudakov form factor that includes the full matrix element for real emission. The truncated shower generates emission at a higher scale (in the evolution variable of the parton shower), while the vetoed shower simulates radiation at a lower evolution scale than the one at which the hardest emission is generated. The POWHEG method has been successfully applied to a wide range of processes [43–62].[2]

These approaches have yet to be applied to processes involving the production of photons due to the complications which arise in the experimental measurement, simulation and calculation at higher orders in perturbation theory of these processes. Collider experiments do not measure *inclusive* photons because of the high background due to the production of photons in meson decays. Indeed, the inclusive production rate of high $p_T$ $\pi^0$, $\eta$, $\omega$ mesons is orders of magnitude bigger than for direct photon production. For this reason the experimental selection of direct photons requires the use of an isolation cut. Different criteria for the isolation of photons include: the cone approach [66, 67], the democratic approach [68] and the smooth isolation procedure [69]. In fixed-order calculations this contribution is included using the measured photon fragmentation function, the probability of a parton fragmenting to produce a photon with a given fraction of the parent parton's momentum, whereas Monte Carlo simulations instead rely on the parton shower and hadronization models to simulate this contribution. This presents a problem in simulating these processes at NLO where some of the singularities in the real emission processes are absorbed into photon fragmentation function in fixed-order calculations. In this paper we will present a method for simulating these processes using the POWHEG approach which still relies on the parton shower and hadronization models to simulate the photon fragmentation contribution. This approach is similar in its philosophy to the method o f ref. [70] for combining leading-order matrix elements and the parton shower.

We illustrate this approach with the simulation of diphoton ($\gamma\gamma$) production. Diphoton production is important as it provides a large background for the discovery of the Higgs boson decaying into a pair of photons, for both the Tevatron [71] and LHC experiments [72, 73]. It is also an important background in new physics models, for example in heavy resonance models [74], models with extra spatial dimensions [75] and cascade decays of heavy new particles [76]. Experimental measurements of $\gamma\gamma$ production have a long history in fixed-target [77–79] and collider experiments [80–84].

The theoretical understanding of diphoton production and precise measurements of the differential cross section are therefore not only important for the discovery of new

[2]There has also been some work combining either many NLO matrix elements [63] or the NLO matrix elements with subsequent emissions matched to leading-order matrix elements [64, 65] with the parton shower.

phenomena but also as a check of the validity of the predictions of perturbative quantum chromodynamics (pQCD) and soft-gluon resummation methods.

The dominant production method for direct photon pairs is leading order $q\bar{q}$ scattering ($q\bar{q} \to \gamma\gamma$), although the formally next-to-next-to-leading-order, $\mathcal{O}(\alpha_s^2)$, gluon-gluon fusion ($gg \to \gamma\gamma$) process via a quark-loop diagram [85] can be important, and even comparable to the leading-order contribution at low diphoton mass ($M_{\gamma\gamma}$) [84], due to the large gluon parton distribution function.

The $\mathcal{O}(\alpha_s)$ corrections to the $q\bar{q} \to \gamma\gamma$ process includes the $q\bar{q} \to \gamma\gamma g$, $gq \to \gamma\gamma q$ and $g\bar{q} \to \gamma\gamma\bar{q}$ processes and corresponding virtual corrections. Moreover, the contribution where the final parton is collinear to a photon is calculated in terms of the quark and gluon fragmentation function into a photon [85, 86]. Given the behaviour of the latter functions, $\sim \frac{\alpha}{\alpha_s}$, these terms contribute to the same order as $q\bar{q} \to \gamma\gamma$.

The calculation of the $\mathcal{O}(\alpha_s)$ corrections to this contribution yield the LO contribution of the double fragmentation type process that corresponds to the case in which both photons are collinear to the final state partons. A full study at NLO accuracy requires that the $\mathcal{O}(\alpha_s)$ corrections to this LO component are in turn calculated. However, the NLO corrections to the fragmentation type contributions are not considered in the present work.

The QCD corrections to the diphoton production process are well known in the literature [66, 87–91]. Fixed-order Monte Carlo programs, such as JETPHOX [92] and DIPHOX [93], provide simulation for direct photon production together with the implementation of isolation cuts.

The present paper is organized as follows. In section 2 we introduce the POWHEG formulae useful for the description of our approach and our treatment of the photon fragmentation contribution. The calculation of the leading-order kinematics with NLO accuracy in the POWHEG approach is discussed in section 3. In section 4 we describe the procedure used to generate the hardest emission. We show our results in section 5 and finally present our conclusions in section 6.

## 2 The POWHEG method

In the POWHEG approach the NLO differential cross section for a given N-body process is

$$\mathrm{d}\sigma = \bar{B}(\Phi_B)\mathrm{d}\Phi_B \left[\Delta_R(0) + \frac{R(\Phi_B,\Phi_R)}{B(\Phi_B)}\Delta_R(k_T(\Phi_B,\Phi_R))\mathrm{d}\Phi_R\right], \tag{2.1}$$

where $\bar{B}(\Phi_B)$ is defined as

$$\bar{B}(\Phi_B) = B(\Phi_B) + V(\Phi_B) + \int \left[R(\Phi_B,\Phi_R) - C(\Phi_B,\Phi_R)\right]\mathrm{d}\Phi_R, \tag{2.2}$$

$B(\Phi_B)$ is the leading-order contribution, $\Phi_B$ the N-body phase-space variables of the LO Born process whereas $\Phi_R$ are the radiative variables describing the phase space for the emission of an extra parton. The real contribution, $R(\Phi_B,\Phi_R)$, is the matrix element including the radiation of an additional parton multiplied by the relevant parton flux factors, and is regulated by subtracting the counter terms $C(\Phi_B,\Phi_R)$ which contain the same singularities as $R(\Phi_B, \Phi_R)$. In practice the counter term is usually composed of a sum over a number of terms, $D^i(\Phi_B, \Phi_R)$, each of which regulates one of the singularities in the matrix element using approaches of either Catani and Seymour (CS) [94] or Frixione, Kunszt and Signer (FKS) [95], i.e. $C(\Phi_B, \Phi_R) = \sum_i D^i(\Phi_B, \Phi_R)$. The finite contribution $V(\Phi_B)$ includes the virtual loop corrections and the counter terms integrated over the real emission variables, which cancel the singularities from the loop corrections, and the collinear remnant from absorbing the initial-state singularities into the parton distribution functions.

The modified Sudakov form factor is defined in terms of the real emission matrix element

$$\Delta_R(p_T) = \exp\left[-\int \mathrm{d}\Phi_R \frac{R(\Phi_B, \Phi_R)}{B(\Phi_B)} \theta(k_T(\Phi_B, \Phi_R) - p_T)\right], \tag{2.3}$$

where $k_T(\Phi_B, \Phi_R)$ is equal to the transverse momentum of the emitted parton in the soft and collinear limits.

The POWHEG method is based on two steps: the N-body configuration is generated according to $\bar{B}(\Phi_B)$ and then the hardest emission is generated using the Sudakov form factor given in eq. (2.3). Since $\bar{B}(\Phi_B)$ is defined as the NLO differential cross section integrated over the radiative variables, the event weight will not be negative.

If the parton shower algorithm is ordered in transverse momentum we would generate the hardest emission first and then evolve the $N+1$ parton final-state system using the shower forbidding any emission with transverse momentum higher than that of the hardest emission. On the contrary for shower simulations which are ordered in other variables, such as angular ordering in Herwig++ [19, 96] , the hardest emission is not necessarily the first one. For this reason the shower must be split into a truncated shower describing soft emission at higher evolution scales, the highest $p_T$ emission and vetoed showers simulating emissions at lower evolution scales; however, constraints are imposed to guarantee that the transverse momentum of the emitted particles is smaller than the one corresponding to the hardest emission [41, 42].

In order to use this procedure for processes involving photons where the real emission matrix elements contain both QCD singularities from the emission of soft and collinear gluons and QED singularities from the radiation of soft and collinear photons we need to make some modifications to the approach. We start by writing the real emission piece as

$$R(\Phi_B, \Phi_R) = R_{\mathrm{QED}}(\Phi_B, \Phi_R) + R_{\mathrm{QCD}}(\Phi_B, \Phi_R), \tag{2.4}$$

where

$$R_{\mathrm{QED}}(\Phi_B, \Phi_R) = \frac{\sum_i D^i_{\mathrm{QED}}}{\sum_j D^j_{\mathrm{QED}} + \sum_j D^j_{\mathrm{QCD}}} R(\Phi_B, \Phi_R) \tag{2.5a}$$

contains the collinear photon emission singularities and

$$R_{\mathrm{QCD}}(\Phi_B, \Phi_R) = \frac{\sum_i D^i_{\mathrm{QCD}}}{\sum_j D^j_{\mathrm{QED}} + \sum_j D^j_{\mathrm{QCD}}} R(\Phi_B, \Phi_R) \tag{2.5b}$$

contains the singularities associated with QCD radiation.[3] Here the counter terms have been split into those $D^i_{\rm QCD}$ which regulate the singularities from QCD radiation and those $D^i_{\rm QED}$ which regulate the singularities due to photon radiation.

We can regard the real QCD emission terms as part of the QCD corrections to the leading-order process, whereas the QED contributions are part of the photon fragmentation contribution coming from a leading-order process with one less photon and an extra parton. We therefore modify the next-to-leading-order cross section for processes with photon production giving

$$\begin{aligned} \mathrm{d}\sigma = & \left\{ B(\Phi_B) + V(\Phi_B) + \int \left[ R_{\rm QCD}(\Phi_B, \Phi_R) - \sum_i D^i_{\rm QCD}(\Phi_B, \Phi_R) \right] \mathrm{d}\Phi_R \right\} \mathrm{d}\Phi_{\rm B} \\ & + R_{\rm QED}(\Phi_B, \Phi_R) \mathrm{d}\Phi_R \mathrm{d}\Phi_{\rm B}. \end{aligned} \tag{2.6}$$

There should also be an additional non-perturbative contribution with the convolution of the photon fragmentation function and the leading-order process with one less photon and an extra parton.

We can now write the cross section for photon production processes in the POWHEG approach in the same way as in eq. (2.1)

$$\begin{aligned} \mathrm{d}\sigma = & \bar{B}(\Phi_B)\mathrm{d}\Phi_B \left[ \Delta_{\rm QCD}(0) + \frac{R_{\rm QCD}(\Phi_B, \Phi_R)}{B(\Phi_B)} \Delta_{\rm QCD}(k_T(\Phi_B, \Phi_R))\mathrm{d}\Phi_R \right] \\ & + B'(\Phi'_B)\mathrm{d}\Phi'_B \left[ \Delta_{\rm QED}(0) + \frac{R_{\rm QED}(\Phi'_B, \Phi'_R)}{B'(\Phi'_B)} \Delta_{\rm QED}(k_T(\Phi'_B, \Phi'_R))\mathrm{d}\Phi'_R \right], \end{aligned} \tag{2.7}$$

where $\bar{B}(\Phi_B)$ is now defined as

$$\bar{B}(\Phi_B) = \left\{ B(\Phi_B) + V(\Phi_B) + \int \left[ R_{\rm QCD}(\Phi_B, \Phi_R) - \sum_i D^i_{\rm QCD}(\Phi_B, \Phi_R) \right] \mathrm{d}\Phi_R \right\} \mathrm{d}\Phi_{\rm B} \tag{2.8}$$

and $B'(\Phi'_B)$ is the leading-order contribution for the process with an extra parton and one less photon with $\Phi'_B$ and $\Phi'_R$ being the corresponding Born and real emission phase-space variables.

The Sudakov form factor for QCD radiation is

$$\Delta_{\rm QCD}(p_T) = \exp\left[ -\int \mathrm{d}\Phi_R \frac{R_{\rm QCD}(\Phi_B, \Phi_R)}{B(\Phi_B)} \theta(k_T(\Phi_B, \Phi_R) - p_T) \right], \tag{2.9a}$$

and the Sudakov form factor for QED radiation is

$$\Delta_{\rm QED}(p_T) = \exp\left[ -\int \mathrm{d}\Phi'_R \frac{R_{\rm QED}(\Phi'_B, \Phi'_R)}{B'(\Phi'_B)} \theta(k_T(\Phi'_B, \Phi'_R) - p_T) \right]. \tag{2.9b}$$

Both the direct photon production and the non-perturbative fragmentation contribution are correctly included. The non-perturbative fragmentation contribution is simulated by the parton shower from the $B'(\Phi'_B)$ contribution when there is no hard QED radiation.

The POWHEG algorithm is implemented for photon production processes using the following procedure.

[3] In practice the counter terms can be negative in some regions and we choose to use their magnitude in this separation in order to ensure that the real contributions are positive.

- First select either a direct photon production or a fragmentation event using $\bar{B}(\Phi_B)$ and $B'(\Phi'_B)$ and the competition method to correctly generate the relative contributions of the two different processes.

- For a direct photon production process:

  - generate the hardest emission using the Sudakov form factor in eq. (2.9a);
  - directly hadronize non-radiative events;
  - map the radiative variables parameterizing the emission into the evolution scale, momentum fraction and azimuthal angle, $(\tilde{q}_h, z_h, \phi_h)$, from which the parton shower would reconstruct identical momenta;
  - generate the $N$-body configuration from $\bar{B}(\Phi_B)$ and evolve the radiating parton from the starting scale down to $\tilde{q}_h$ using the truncated shower;
  - insert a branching with parameters $(\tilde{q}_h, z_h, \phi_h)$ into the shower when the evolution scale reaches $\tilde{q}_h$;
  - generate $p_T$ vetoed showers from all the external legs.

- For a fragmentation contribution:

  - generate the hardest QED emission using the Sudakov form factor in eq. (2.9b);
  - directly shower and hadronize non-radiative events, forbidding any perturbative QED radiation in the parton shower generating the non-perturbative fragmentation contribution;
  - for events with QED radiation map the radiative variables parameterizing the emission into the evolution scale, momentum fraction and azimuthal angle, $(\tilde{q}_h, z_h, \phi_h)$, from which the parton shower would reconstruct identical momenta;
  - generate the $N$-body configuration from $B'(\Phi'_B)$ and evolve the radiating parton from the starting scale down to $\tilde{q}_h$ using the truncated shower, but allowing QCD radiation with $p_T$ greater than that of the hardest QED emission;
  - insert a branching with parameters $(\tilde{q}_h, z_h, \phi_h)$ into the shower when the evolution scale reaches $\tilde{q}_h$;
  - generate the shower from all external legs forbidding QED radiation, but not QCD radiation, above the $p_T$ of the hardest emission.

This procedure now includes the QCD corrections to the leading-order direct photon production process and both the perturbative QED corrections to the photon fragmentation contribution and the non-perturbative contribution are simulated by the parton shower.

In the next two sections we will describe how we implement this approach in Herwig++ for photon pair production.

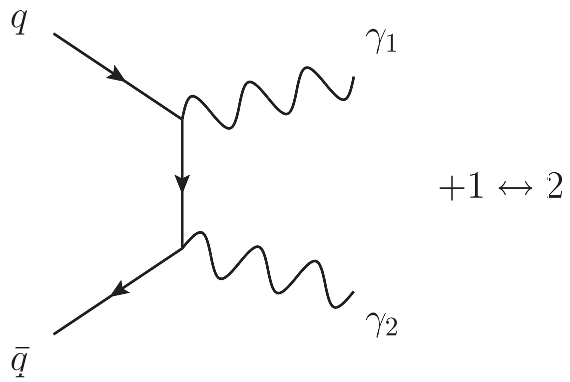


**Figure 1**. Diphoton production at leading-order.

## 3 Calculation of $\bar{B}(\Phi_B)$

In this section we describe the $\mathcal{O}(\alpha_s)$ corrections to diphoton production. At leading-order, $\gamma\gamma$-production is described by the Feynman diagram illustrated in figure 1. Next-to-leading-order contributions yield $\mathcal{O}(\alpha_s)$ corrections coming from $q\bar{q} \to \gamma\gamma g$, $gq \to \gamma\gamma q$ and $g\bar{q} \to \gamma\gamma\bar{q}$, together with the corresponding virtual corrections, as shown in figure 2. These subprocesses contain QED singularities, corresponding to configurations where the final-state parton becomes collinear to a photon, which do not cancel when summing up the real and the virtual pieces of the cross section. As described in the previous section they are formally absorbed into a quark ($G_{\gamma q}(z,\mu^2)$) or gluon ($G_{\gamma g}(z,\mu^2)$) fragmentation function into photons, which define the probability of finding a photon carrying longitudinal momentum fraction $z$ in a quark or gluon jet at scale $\mu$ for a given factorization scheme. This QED singular component is called the *Bremsstrahlung* or single fragmentation contribution. In our approach it is treated separately and simulated by showering the $gq \to \gamma q$ or $g\bar{q} \to \gamma\bar{q}$ within the Monte Carlo algorithm, see figure 3, as described in the previous section. At next-to-leading-order the same configuration appears in any subprocess in which a quark (gluon) undergoes a cascade of successive collinear splittings ending up with a quark-photon (gluon-photon) splitting. These singularities are factorized to all orders in $\alpha_s$, according to the factorization theorem. When the fragmentation scale $\mu$ is chosen higher than any other hadronic scale, i.e. $\mu \sim 1\,\mathrm{GeV}$, these functions behave roughly as $\frac{\alpha}{\alpha_s(\mu^2)}$ and therefore they contribute at leading-order.

For a full study at NLO accuracy, the $\mathcal{O}(\alpha_s)$ corrections to the Bremsstrahlung contribution need to be calculated. Moreover, these corrections in their turn yield the leading-order contribution of the double fragmentation type process; in the latter case, both photons result from the collinear fragmentation of a parton. However, these corrections are out of the scope of the present work and are not considered here.

### 3.1 Real emission contribution

In order to calculate the real emission contribution to $\bar{B}(\Phi_B)$ we need to specify both the radiative phase space, $\Phi_R$, and the subtraction counter terms. We choose to use the dipole subtraction algorithm of Catani and Seymour [94] to specify the counter terms and the associated definition of the real emission phase space as follows.

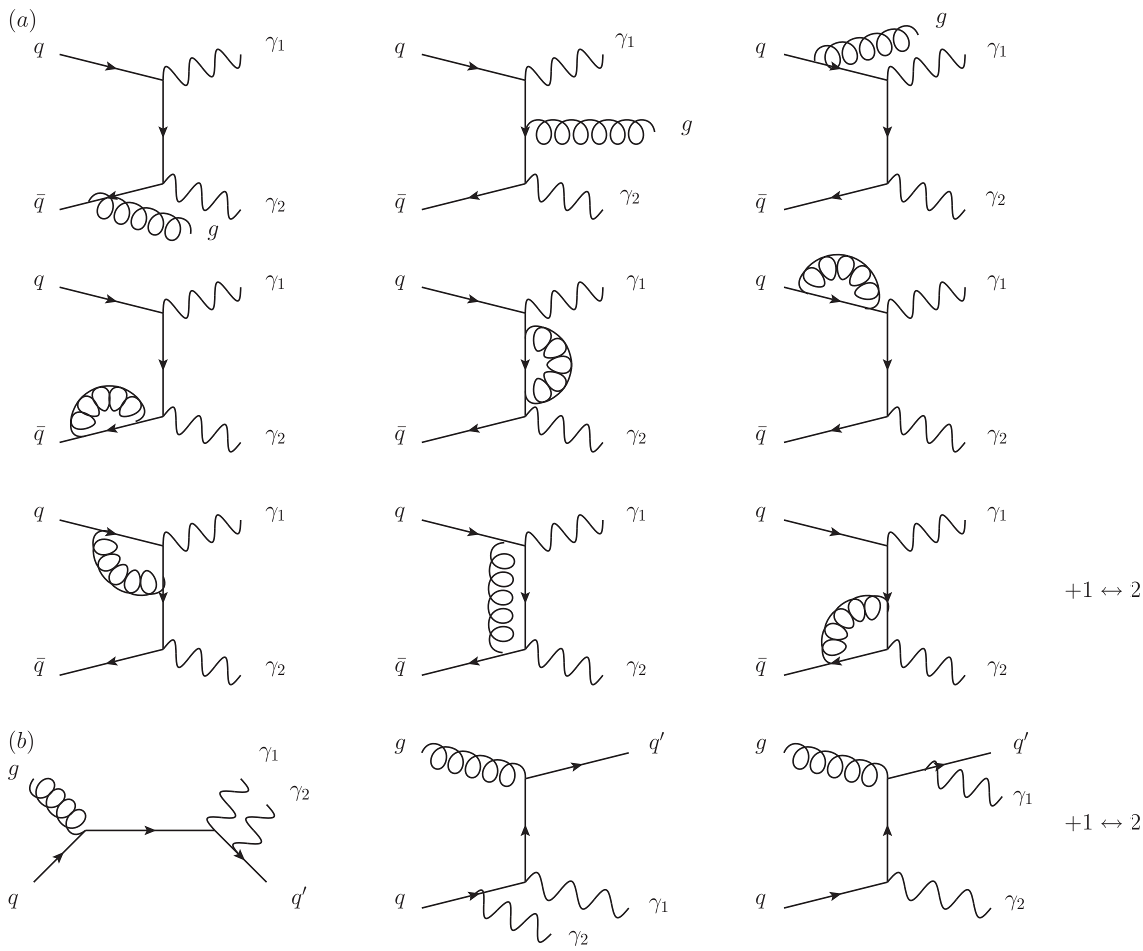


**Figure 2**. Diphoton production at next-to-leading-order. In (a) the real and virtual Feynman diagrams contributing to the $q\bar{q} \to \gamma\gamma$ subprocess are shown while in (b) the real diagrams for $gq$ initiated process are given.

In the centre-of-mass frame the incoming hadronic momenta are, $P_\oplus$ and $P_\ominus$, respectively for the hadrons traveling in the positive and negative $z$-directions. Similarly the momenta of the incoming partons in the Born process are $\bar{p}_\oplus = \bar{x}_\oplus P_\oplus$ and $\bar{p}_\ominus = \bar{x}_\ominus P_\ominus$, respectively. The momenta of the photons in the Born process are $\bar{k}_{1,2}$ respectively. The corresponding momenta in the real emission process are $p_\oplus$ and $p_\ominus$ for the incoming partons and $k_{1,2,3}$ for the outgoing particles which are chosen such that $k_{1,2}$ are the momenta of the photons and $k_3$ that of the radiated final-state parton.

In the CS approach the real phase space depends on which parton is the emitter of the radiation and which the associated spectator defining the dipole [94]. When the parton with momentum $\bar{p}_\oplus$ is the emitter and that with momenta $\bar{p}_\ominus$ the spectator the full phase space is [94]

$$\mathrm{d}\Phi_3 = \mathrm{d}\Phi_B \mathrm{d}\Phi_R = \mathrm{d}\Phi_B \frac{(k_1+k_2)^2}{16\pi^2}\,\frac{d\phi_\oplus}{2\pi}\,dv_\oplus\,\frac{dx}{x}\,\theta(v_\oplus)\,\theta\left(1-\frac{v_\oplus}{1-x}\right)\theta(x(1-x))\,\theta(x-\bar{x}_\oplus), \tag{3.1}$$

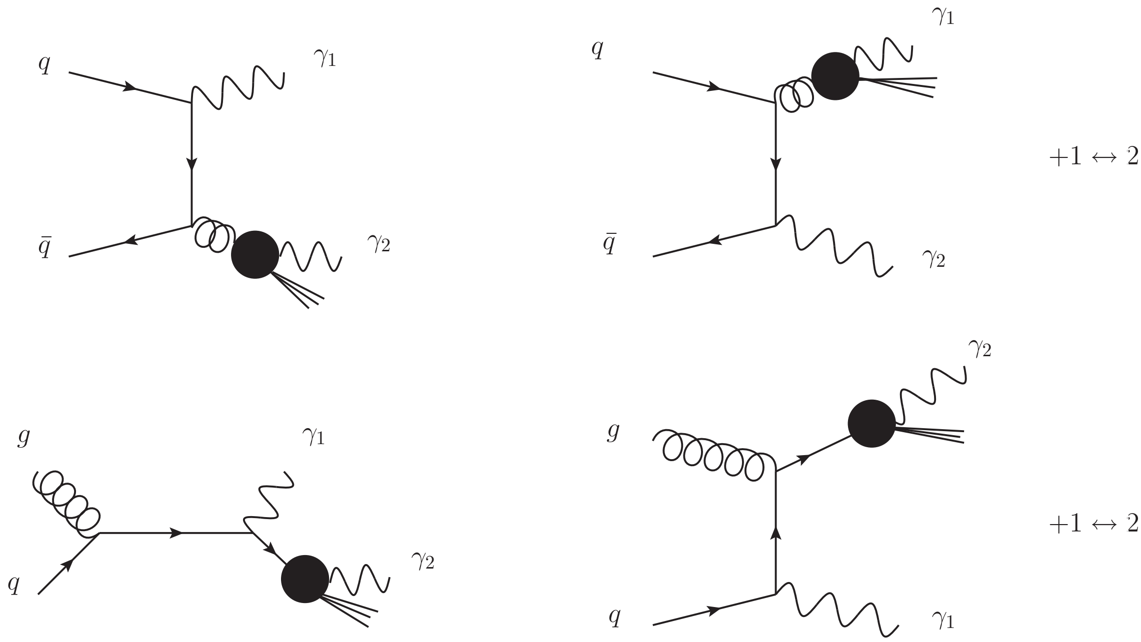


**Figure 3**. Bremsstrahlung contribution for diphoton production.

where the radiative phase space variables are

$$x = 1 - \frac{(p_\oplus + p_\ominus)\cdot k_3}{p_\oplus \cdot p_\ominus}, \qquad v_\oplus = \frac{p_\oplus \cdot k_3}{p_\oplus \cdot p_\ominus}, \qquad \phi_\oplus, \tag{3.2}$$

$\phi_\oplus$ is the azimuthal angle of the emitted particle around the $\hat{\oplus}$-direction and

$$x \in [x_\oplus, 1], \qquad v_\oplus \in [0, 1-x]. \tag{3.3}$$

In terms of these variables

$$p_\oplus = \bar{p}_\oplus / x, \qquad p_\ominus = \bar{p}_\ominus, \tag{3.4a}$$

$$x_\oplus = \bar{x}_\oplus / x, \qquad x_\ominus = \bar{x}_\ominus. \tag{3.4b}$$

It is useful to specify the momentum of the radiated parton in terms of its transverse momentum, $p_T$, and rapidity, $y$, such that

$$k_3 = p_T \left(\cosh y; \cos\phi_\oplus, \sin\phi_\oplus, \sinh y\right). \tag{3.5}$$

Using the definition of $x$ and $v_\oplus$ we have

$$k_3 = v_\oplus p_\ominus + (1 - x - v_\oplus) p_\oplus + q_\perp, \tag{3.6}$$

where $q_\perp$ is the component of the 4-momenta transverse to the beam direction. The on-shell condition, $k_3^2 = 0$, gives

$$-q_\perp^2 = p_T^2 = 2 p_\oplus \cdot p_\ominus (1 - x - v_\oplus) v_\oplus. \tag{3.7}$$

From eq. (3.6) and the definition of rapidity

$$y = \frac{1}{2}\ln\left[\frac{k_3^E + k_3^z}{k_3^E - k_3^z}\right] = \frac{1}{2}\ln\left[\frac{(1-x-v_\oplus)x_\oplus}{v_\oplus x x_\ominus}\right], \tag{3.8}$$

the CS variables are

$$\begin{cases} v_\oplus = \frac{1}{x_\ominus\sqrt{s}} p_T e^{-y}, \\ x = \frac{1-\frac{p_T}{x_\ominus\sqrt{s}}e^{-y}}{1+\frac{p_T}{x_\oplus\sqrt{s}}e^{y}}. \end{cases} \tag{3.9}$$

This is sufficient to calculate the momentum of the radiated parton, however, rather than implementing the real emission variables in the Sudakov form factor in this way and then imposing the $\theta(k_T(\Phi_B, \Phi_R) - p_T)$ function it is easier to consider the real emission in terms of the transverse momentum, rapidity and azimuthal angle of the emitted parton.

The Jacobian for this transformation is

$$\left|\frac{\partial(x,v)}{\partial p_T \partial y}\right| = \frac{\frac{2p_T}{s x_\oplus x_\ominus}\left(1 - \frac{p_T}{\sqrt{s}x_\ominus}e^{-y}\right)}{\left(1 + \frac{p_T}{\sqrt{s}x_\oplus}e^{y}\right)^2} = \frac{2p_T x^2}{s x_\oplus x_\ominus (1-v_\oplus)}. \tag{3.10}$$

The momenta of the photons in the real emission process can then be calculated from the Born momenta using

$$k_r^\mu = \Lambda^\mu{}_\nu \bar{k}_r^\nu \qquad r = 1,2, \tag{3.11}$$

where the Lorentz transformation is

$$\Lambda^\mu{}_\nu = g^\mu{}_\nu - \frac{2(K+\bar{K})^\mu (K+\bar{K})_\nu}{(K+\bar{K})^2} + \frac{2K^\mu \bar{K}_\nu}{K^2}, \tag{3.12}$$

with

$$K = p_\oplus + p_\ominus - k_3 = k_1 + k_2, \tag{3.13a}$$

$$\bar{K} = \bar{p}_\oplus + \bar{p}_\ominus. \tag{3.13b}$$

The condition $K^2 = \bar{K}^2$ is compatible with the definition of $x$ given in eq. (3.2). The kinematic variables for the $\hat{\ominus}$ collinear direction are calculated in a similar way and they provide a radiative phase space as in eq. (3.1). Moreover, given the $x_\oplus \leftrightarrow x_\ominus$ asymmetry of the rapidity in eq. (3.8), it is $[y]_\ominus = -[y]_\oplus$. In the rest of the paper we refer to the collinear direction as $\hat{\mathrm{O}} = \{\hat{\ominus}, \hat{\oplus}\}$, when both components need to be included.

In addition to the real emission variables we need the dipole subtraction terms of ref. [94]. In the following $B(\Phi_B)$ and $B'(\Phi'_B)$ are computed in terms of the reduced momenta defined in terms of the momenta for the real emission process in ref. [94]. The QCD singularities from $q\bar{q} \to \gamma\gamma g$ are absorbed by the dipoles

$$D^{qg,\bar{q}} \equiv D^{qg}_{\mathrm{QCD}} = 8\pi C_F \alpha_s(\mu_R) \frac{1}{2\bar{p}_\oplus k_3}\left\{\frac{2}{1-x} - (1+x)\right\} B(\Phi_B), \tag{3.14a}$$

$$D^{\bar{q}g,q} \equiv D^{\bar{q}g}_{\mathrm{QCD}} = 8\pi C_F \alpha_s(\mu_R) \frac{1}{2\bar{p}_\ominus k_3}\left\{\frac{2}{1-x} - (1+x)\right\} B(\Phi_B), \tag{3.14b}$$

where the dipoles $D^{ij,k}$ denote the emitter $i$, emitted parton $j$ and spectator $k$.

The $gq \to \gamma\gamma q$ subprocess involves the QCD dipoles

$$D^{gq,q} \equiv D^{gq}_{\rm QCD} = 8\pi T_F \alpha_s(\mu_R) \frac{1}{2\bar{p}_\oplus k_3} \left\{1 - 2x(1-x)\right\} B(\Phi_B). \tag{3.15}$$

In order to separate the QCD and QED emission we also need the QED dipoles

$$D^{q}_{q\gamma} \equiv D^{q\gamma F}_{\rm QED} = 8\pi\alpha e_q^2 \frac{1}{2k_2 k_3 \xi} \left\{\frac{2}{1-\xi+z} - 2 + z\right\} B'(\Phi'_B), \tag{3.16a}$$

$$D^{q\gamma}_{q} \equiv D^{q\gamma I}_{\rm QED} = 8\pi\alpha e_q^2 \frac{1}{2p_\ominus k_3 \xi} \left\{\frac{2}{1-\xi+z} - (1+x)\right\} B'(\Phi'_B), \tag{3.16b}$$

where

$$\xi = 1 - \frac{k_2 k_3}{(k_2+k_3)p_\oplus}, \tag{3.17a}$$

$$z = \frac{p_\oplus k_2}{(k_2+k_3)p_\oplus}, \tag{3.17b}$$

and $e_q$ is the charge of the quark $q$ in units of the electron charge. In this case, the radiative phase space is $\mathrm{d}\Phi'_R(\xi, z, \phi')$. Similar dipoles are included for the $g\bar{q} \to \gamma\gamma\bar{q}$ subprocess. We do not include perturbative QED radiation from the $q\bar{q} \to \gamma g$ subprocess as it does not give a perturbative correction to $G_{\gamma g}(z, \mu^2)$.

In practice we generate the real emission piece as a contribution from each of the incoming partons as

$$\int \left[R_{\rm QCD}(\Phi_B, \Phi_R) - \sum_i D^i_{\rm QCD}(\Phi_B, \Phi_R)\right] \mathrm{d}\Phi^i_R =$$

$$\sum_{i=\oplus,\ominus} \int \left[\frac{|D^i_{\rm QCD}|}{\sum_j |D^j_{\rm QED}| + \sum_j |D^j_{\rm QCD}|} R(\Phi_B, \Phi^i_R) - D^i_{\rm QCD}(\Phi_B, \Phi_R)\right] \mathrm{d}\Phi^i_R. \tag{3.18}$$

For the later generation of the Sudakov form factor it is useful to express the dipoles as

$$D^I_{\rm QCD} \equiv \frac{\mathcal{C}_I \alpha_s(\mu_R)}{2\pi} \mathcal{D}^I B(\Phi_B), \tag{3.19}$$

where $I = \{qg; \bar{q}g; gq; g\bar{q}\}$,

$$\mathcal{C}_{qg} = \mathcal{C}_{\bar{q}g} = C_F, \tag{3.20a}$$

$$\mathcal{C}_{gq} = \mathcal{C}_{g\bar{q}} = T_F, \tag{3.20b}$$

and

$$D^J_{\rm QED} \equiv \frac{\alpha}{2\pi} e_q^2 \mathcal{D}_J B(\Phi'_B), \tag{3.21}$$

where $J = \{q\gamma F, q\gamma I, \bar{q}\gamma F, \bar{q}\gamma I\}$.



JHEP02(2012)130

### 3.2 Virtual contribution and collinear remainders

The finite piece of the virtual correction is

$$d\sigma_V = \frac{C_F\alpha_s(\mu_R)}{2\pi}V(w)B(\Phi_B). \tag{3.22}$$

where the finite contribution of $\mathbf{I}(\epsilon)$ [94] and the virtual correction [89] is

$$V(w) = \left(3+\ln^2 w+\ln^2(1-w)+3\ln(1-w)\right)+\frac{F(w)}{\left(\frac{1-w}{w}+\frac{w}{1-w}\right)}, \tag{3.23}$$

where $e_q$ is the electric charge of quark $q$, and

$$\begin{aligned} F(w) &= 2\ln w+2\ln(1-w)+\frac{3(1-w)}{w}(\ln w-\ln(1-w)) \\ &\quad+\left(2+\frac{w}{1-w}\right)\ln^2 w+\left(2+\frac{1-w}{w}\right)\ln^2(1-w), \end{aligned} \tag{3.24}$$

with $w = 1+\frac{\hat{t}}{\hat{s}}$, where $\hat{s}$ and $\hat{t}$ are the usual Mandelstam variables.

The collinear remainders are

$$d\sigma_{\text{coll}} = \frac{C_F\alpha_s(\mu_R)}{2\pi}\frac{f^m(x_{\text{O}},\mu_F)}{f(x_{\text{O}},\mu_F)}B(\Phi_B), \tag{3.25}$$

where the modified PDF is[4]

$$\begin{aligned} f_q^m(x_{\text{O}},\mu_F) &= \int_{x_{\text{O}}}^1 \frac{dx}{x}\left\{f_g\left(\frac{x_{\text{O}}}{x},\mu_F\right)A(x)\right. \\ &\quad+\left[f_q\left(\frac{x_{\text{O}}}{x},\mu_F\right)-xf_q(x_{\text{O}},\mu_F)\right]B(x) \\ &\quad\left.+f_q\left(\frac{x_{\text{O}}}{x},\mu_F\right)C(x)\right\}+f_q(x_{\text{O}},\mu_F)D(x_{\text{O}}), \end{aligned} \tag{3.26}$$

$f_q$ and $f_g$ are the quark and gluon PDFs respectively, and

$$A(x) = \frac{T_F}{C_F}\left[2x(1-x)+(x^2+(1-x)^2)\ln\frac{Q^2(1-x)^2}{\mu_F^2 x}\right], \tag{3.27}$$

$$B(x) = \left[\frac{2}{1-x}\ln\frac{Q^2(1-x)^2}{\mu_F^2}\right], \tag{3.28}$$

$$C(x) = \left[1-x-\frac{2}{1-x}\ln x-(1+x)\ln\frac{Q^2(1-x)^2}{\mu_F^2 x}\right], \tag{3.29}$$

$$D(x_{\text{O}}) = \left[\frac{3}{2}\ln\left(\frac{Q^2}{\mu_F^2}\right)+2\ln(1-x_{\text{O}})\ln\left(\frac{Q^2}{\mu_F^2}\right)+2\ln^2(1-x_{\text{O}})+\frac{\pi^2}{3}-5\right]. \tag{3.30}$$

The combined contribution of the finite virtual term and collinear remnants is

$$d\sigma_{V+\text{coll}} = \frac{C_F\alpha_s(\mu_R)}{2\pi}\mathcal{V}(\Phi_B)B(\Phi_B), \tag{3.31}$$

where

$$\mathcal{V}(\Phi_B) \equiv V(w)+\tilde{V}(x_{\text{O}},\mu_F), \tag{3.32}$$

with $\tilde{V}(x_{\text{O}},\mu_F) = \frac{f^m(x_{\text{O}},\mu_F)}{f(x_{\text{O}},\mu_F)}$.

[4] We write the modified PDF for the quark $q$, but a similar expression is valid for an incoming antiquark $\bar{q}$.



JHEP02(2012)130

### 3.3 Generation of the hard process

The next-to-leading-order simulation of photon pair production in Herwig++ uses the standard Herwig++ machinery to generate photon pair and photon plus jet production in competition. The $\bar{B}$ function is implemented as a reweighting of the leading-order matrix element as follows:

1. the radiative variables $\Phi_R\{x, v, \phi\}$ and $\Phi'_R\{\xi, z, \phi'\}$ are transformed into a new set such that the radiative phase space is a unit volume;

2. using the standard Herwig++ leading-order matrix element generator, we generate a leading-order configuration and provide the Born variables $\Phi_B$ with an associated weight $B(\Phi_B)$;

3. the radiative variables $\Phi_R$ are generated and $\bar{B}(\Phi_B)$ sampled in terms of the unit cube $(\tilde{x}, \tilde{v}, \tilde{\phi})$, using the Auto-Compensating Divide-and-Conquer (ACDC) phase-space generator [97];

4. the leading-order configuration is accepted with a probability proportional to the integrand of eq. (2.8) evaluated at $\{\Phi_B, \Phi_R\}$.

## 4 The generation of the hardest emission

Following the generation of the Born kinematics with next-to-leading-order accuracy the hardest QCD or QED emission must be generated according to eqs. (2.9a) or (2.9b), respectively depending on whether a direct or photon fragmentation contribution was selected.

### 4.1 The hardest QED emission

The hardest QED emission is generated by using the modified Sudakov form factor defined in eq. (2.9b). We generate it in terms of the variables $\Phi'_R(x_p, z_p, \phi)$, with

$$\mathrm{d}\Phi'_R = \frac{1}{2\pi}\mathrm{d}x_p\mathrm{d}z_p\mathrm{d}\phi, \tag{4.1}$$

defined in [9, 13], where $x_p \in [x_o, 1]$, $z_p \in [0, 1]$ and the azimuthal angle $\phi \in [0, 2\pi]$. The invariant mass of the initial-final dipole $q^2 = (p_i - p_k)^2 = -Q^2$ is preserved by the photon radiation. It is easiest to generate the hardest emission by introducing $x_\perp$ such that the transverse momentum of the emission relative to the direction of the partons in the Breit frame of the dipole is $p_T = \frac{Q}{2}x_\perp$, where

$$x_\perp^2 = \frac{4(1-x_p)(1-z_p)z_p}{x_p}. \tag{4.2}$$

The Sudakov form factor can then be calculated in terms of $\tilde{\Phi}'_R(x_\perp, z_p, \phi)$, such that the $\theta$-function simply gives $x_\perp$ as integration limits and eq. (2.9b) becomes

$$\Delta^J_{\mathrm{QED}}(x_\perp) = \exp\left(-\int_{x_\perp}^{x_\perp^{\max}} \frac{\mathrm{d}x'_\perp}{x'^3_\perp}\mathrm{d}\phi\mathrm{d}z_p \frac{\alpha}{2\pi}\mathcal{W}\frac{\mathcal{A}^J_{\mathrm{QED}}}{B}\right), \tag{4.3}$$

where

$$\frac{\alpha}{2\pi}\mathcal{A}^J_{\mathrm{QED}} = \frac{|D^J_{\mathrm{QED}}|}{\sum_j |D^j_{\mathrm{QED}}| + \sum_j |D^j_{\mathrm{QCD}}|} R(\Phi_B, \Phi^J_R), \tag{4.4}$$

the Jacobian, $\mathcal{W}$, is

$$\mathcal{W} = 4z_p(1-z_p)(1-x_p)^2, \tag{4.5}$$

and $\frac{Q}{2}x_\perp^{\max}$ is the maximum value for the transverse momentum.

It is impossible to generate the hardest emission directly using eq. (4.3) instead we use an overestimate

$$g(x_\perp) = \frac{a}{x_\perp^3}, \tag{4.6}$$

of the integrand in eq. (4.3) so that

$$\Delta^{\mathrm{over}}_{\mathrm{QED}}(x_\perp) = \exp\left(-\int_{x_\perp}^{x_\perp^{\max}} \frac{\mathrm{d}x'_\perp}{x'^3_\perp} \mathrm{d}\phi \mathrm{d}z_p a\right) \tag{4.7}$$

can be easily integrated in $\{x_\perp, x_\perp^{\max}\}$. This allows us to solve $\mathcal{R}_1 = \Delta^{\mathrm{over}}_{\mathrm{QED}}(x_\perp)$ where $\mathcal{R}_1$ is a random number in $[0,1]$ to get the transverse momentum of a trial hard emission

$$x_\perp^2(\mathcal{R}_1) = \frac{1}{\frac{1}{(x_\perp^{\max})^2} - \frac{2}{a}\ln \mathcal{R}_1}. \tag{4.8}$$

This trial hard emission is then accepted or rejected using a probability given by the ratio of the true integrand to the overestimated value. If the emission is rejected the procedure is repeated with $x_\perp^{\max}$ set to the rejected $x_\perp$ value until the generated value is below the cut-off. This procedure, called the *veto algorithm*, correctly generates the hardest emission according to eq. (4.3) [98].

### 4.2 The hardest QCD emission

The hardest QCD emission is generated in terms of the variables $\Phi_R(p_T, y, \phi)$ defined in section 3.1. Eq. (2.9a) then becomes

$$\Delta^I_{\mathrm{QCD}}(p_T) = \exp\left(-\int_{p_T}^{p_T^{\max}} \mathrm{d}p'_\perp \mathrm{d}\phi \mathrm{d}y \frac{\mathcal{C}_I \alpha_s}{2\pi}\mathcal{W}_I \frac{\mathcal{A}^I_{\mathrm{QCD}}}{B}\right), \tag{4.9}$$

where

$$\frac{\mathcal{C}_I\alpha_s}{2\pi}\mathcal{A}^I_{\mathrm{QCD}} = \frac{|D^I_{\mathrm{QCD}}|}{\sum_j |D^j_{\mathrm{QED}}| + \sum_j |D^j_{\mathrm{QCD}}|} R(\Phi_B, \Phi^I_R), \tag{4.10}$$

the Jacobian is

$$\mathcal{W}_I = \frac{x}{1 - v_{\mathrm{O}}}, \tag{4.11}$$

where we mean to use $v_\oplus$ for $I = \{qg; gq; g\bar{q}\}$ and $v_\ominus$ for $I = \{\bar{q}g\}$.

As before we use the veto algorithm to generate the hardest QCD emission according to eq. (4.9). In this case we introduce the overestimate function

$$g_I(p_T) = \frac{a_I}{p_T}, \tag{4.12}$$

so that

$$\Delta^{\rm over}_{\rm QCD}(p_T) = \exp\left(-\int_{p_T}^{p_T^{\rm max}} \frac{{\rm d}p'_T}{p'_T}{\rm d}\phi{\rm d}y a_I\right) \tag{4.13}$$

is easily integrable in $\{p_T, p_T^{\rm max}\}$ and $\mathcal{R}_1 = \Delta^{\rm over}_{\rm QCD}(p_T)$ can be solved giving

$$p_T(\mathcal{R}_1) = \mathcal{R}_1^{\frac{1}{a}}. \tag{4.14}$$

As before this trial hard emission is then accepted or rejected using a probability given by the ratio of the true integrand to the overestimated value. If the emission is rejected the procedure is repeated with $p_T^{\rm max}$ set to the rejected $p_T$ value until the generated value is below the cut-off.

## 5 Results

Unlike the implementations of many other processes in the POWHEG formalism it is impossible to directly compare our results for any quantities directly with next-to-leading-order simulations in order to test the implementation due to the very different treatment of the photon fragmentation contribution. Instead we compare a simple observable, the rapidity of the photons, with the next-to-leading-order program DIPHOX [93] as a sanity check of our results not expecting exact agreement, although the PDFs and electroweak parameters were chosen to give exact agreement for the leading order $q\bar{q} \to \gamma\gamma$ process.

For proton-proton collisions at a centre-of-mass energy of 14 TeV, we used the following set of cuts on $p_T$ and rapidity of photons

$$p_T^\gamma > 25 \text{ GeV}, \qquad\qquad |y^\gamma| < 2.5, \tag{5.1}$$

together with a cut on the invariant mass of the $\gamma\gamma$-pair

$$80 \text{ GeV} < M^{\gamma\gamma} < 1500 \text{ GeV}. \tag{5.2}$$

Moreover, we follow typical experimental selection cuts to isolate direct photons from the background: we require that the amount of total transverse energy, $E_T^{\rm had}$, released in the cone, centred around the photon direction in the rapidity and azimuthal angle plane, is smaller than 15 GeV, i.e.

$$(y - y^\gamma)^2 + (\phi - \phi^\gamma)^2 \leq R^2 \tag{5.3}$$

$$E_T^{\rm had} \leq 15 \text{ GeV}, \tag{5.4}$$

where $R = 0.4$ is the radius of the cone. The PDFs are chosen to be the CTEQ6 set [99]. The result is shown in figure 4. The distributions from DIPHOX at NLO(red dashed line) and LO (red dash-dotted line), together with LO Herwig++ (dotted black line) and Herwig++ with POWHEG corrections (solid black line) do not include the gluon-gluon channel. At LO the Herwig++ and DIPHOX distributions are indistinguishable. At NLO they show a difference that is very small compared to the correction from LO to NLO, which means that the NLO curves are in reasonable agreement given the sizable contribution of

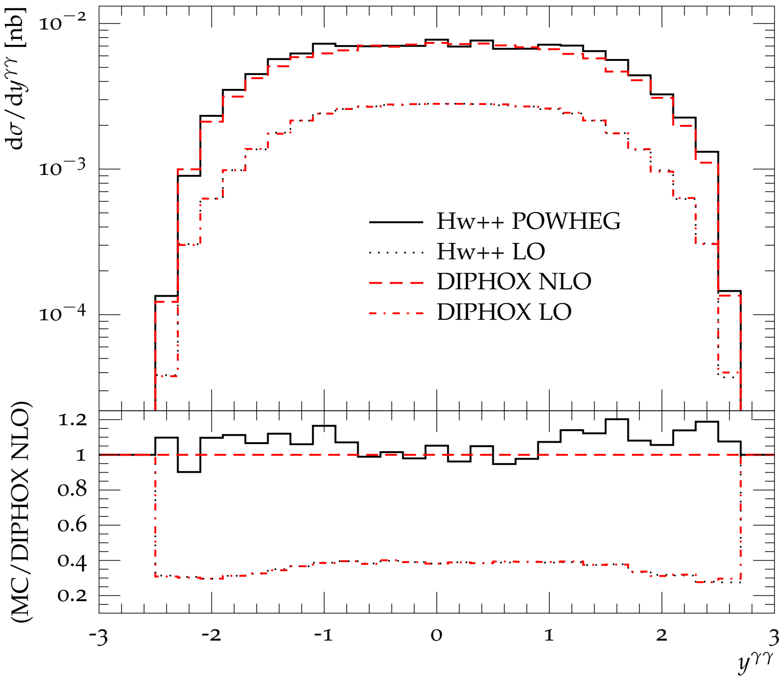


**Figure 4**. Rapidity of the $\gamma\gamma$-pair at NLO. The distribution from the Herwig++ parton shower with POWHEG correction (solid black line) is compared with NLO cross section from DIPHOX (dashed red line). At LO the Herwig++ distribution is given by the dotted black line while the cross section from DIPHOX by the dash-dotted red line. In the lower panel we show the ratio of each distribution (MC) over the DIPHOX curve at NLO.

the fragmentation contribution that is treated differently in the two approaches. The size of the difference of the two approaches is better seen in the lower panel that shows ratio plot of each distribution (MC) over the DIPHOX curve at NLO.

In figure 5a we compare the results from Herwig++ with the data of ref. [83], a fixed next-to-leading-order calculation from DIPHOX (dotted magenta line) and RESBOS (dashed-dotted green line) [100–104], which performs an analytic resummation of the logarithmically enhanced contributions. Here and in the following the LO Herwig++ parton shower (red dashed line) includes the $q\bar{q} \to \gamma\gamma$, $qg \to \gamma$jet and $gg \to \gamma\gamma$ contribution. The implementation of POWHEG correction improves the description and this results in a distribution (solid blue line) that is in good agreement with the data. Here, as in the following, the NLO curve includes the $gg \to \gamma\gamma$ subprocess. In the lower frame, we plot the ratio MC/data and the yellow band gives the one sigma variation of data. All the plots comparing the results of Herwig++ with experimental results were made using the Rivet [105] package.

It is of interest to study the transverse momentum of the $\gamma\gamma$-pair, because it is not infrared safe for $p_\perp^{\gamma\gamma} \to 0$. The $q\bar{q} \to \gamma\gamma$ and $gg \to \gamma\gamma$ processes present a loss of balance between the corresponding real emission and virtual contribution, which results in large logarithms at every order in perturbation theory. In addition, the fragmentation compo-

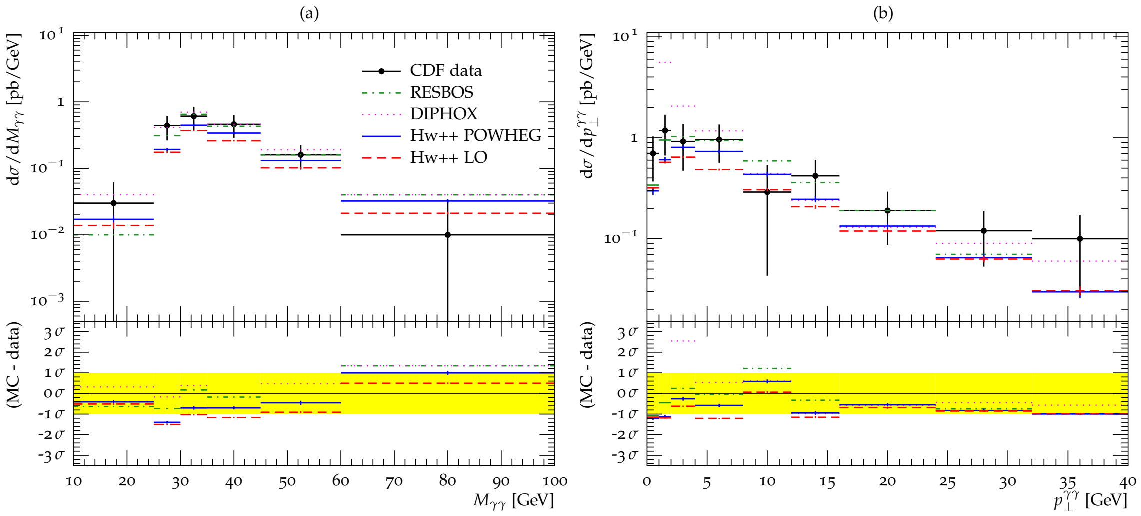


**Figure 5**. The (a) invariant mass and (b) transverse momentum of the $\gamma\gamma$-pair. The solid blue line shows the POWHEG approach, while the dashed red curve shows the result of the Herwig++ shower at LO. We show the NLO cross section provided by DIPHOX (magenta dotted line) and RESBOS (green dashed-dotted line). The data are from ref. [83] and the curves are plotted with Rivet [105]. In the lower panel, the yellow band describes the one sigma variation of data.

nents introduce an extra convolution that smears out this singularity. Since DIPHOX is based on a fixed, finite order calculation it is not suitable for the study of infrared sensitive observables and it fails in the description of these observables at low $p_\perp^{\gamma\gamma}$, as it is shown in figure 5b (dotted magenta line). Resummation for diphoton production in hadron-hadron collision has been provided at all orders in $\alpha_s$ in ref. [106] and implemented in RESBOS, as the corresponding distribution (dashed-dotted green line) shows in the same figure. The Herwig++ parton shower resums the effect of enhanced collinear emission to all orders in $\alpha_s$ in the leading-logarithmic (LL) approximation and results in a finite behaviour for $p_\perp^{\gamma\gamma} \to 0$ (red dashed line). However, the LO distribution does not correctly describe the data. In presence of POWHEG correction the distribution (solid blue line) stays finite at low $p_\perp^{\gamma\gamma}$ and is in good agreement with the CDF data [83].

In addition, Herwig++ distributions, with and without POWHEG corrections, are compared to the data of ref. [84]. In figure 6, we show the transverse momentum of the diphoton pair for two ranges of invariant mass of the $\gamma\gamma$-pair, $M_{\gamma\gamma}$; in figure 6a 50 GeV $< M_{\gamma\gamma} <$ 80 GeV and in figure 6b 80 GeV $< M_{\gamma\gamma} <$ 350 GeV. For the same ranges of $M_{\gamma\gamma}$ we plot the azimuthal angle distribution between the photons in figure 7a and figure 7b respectively and the polar angle between the photons in figure 8a and figure 8b. For all distributions we see that the LO Herwig++ ditributions (red dashed line) do not correctly describe the data. The POWHEG approach improves the simulation and provides a good description of D0 data [84].

To estimate the effect of our implementation on theoretical uncertainties, we plot scale variation for the azimuthal angle distribution between the photons with 50 GeV $< M_{\gamma\gamma} <$ 80 GeV (figure 9). The scale variation is between 1/2 and twice the scale for the bands

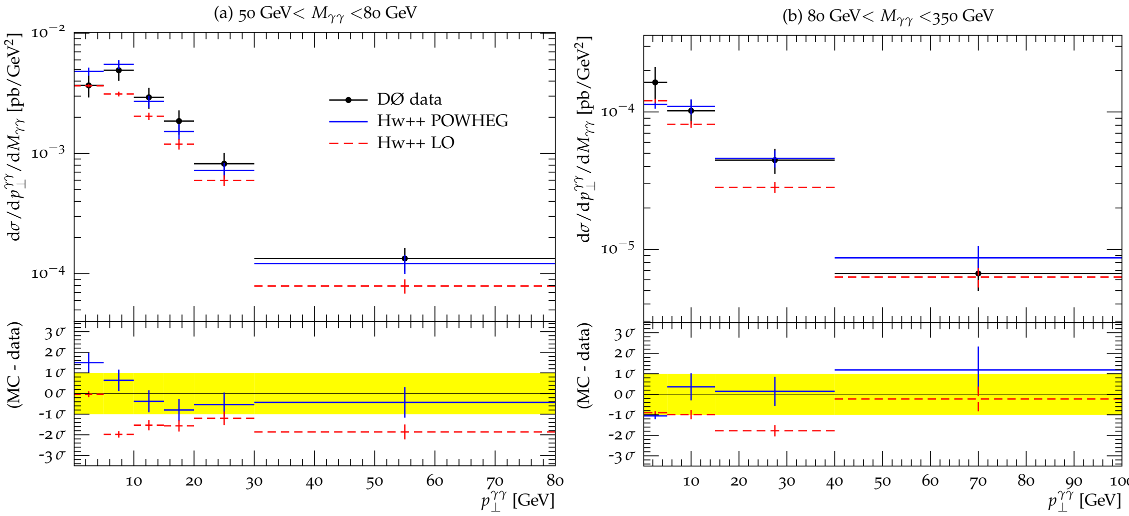


**Figure 6**. Transverse momentum of the diphoton system for (a) 50 GeV $< M_{\gamma\gamma} <$ 80 GeV and (b) 80 GeV $< M_{\gamma\gamma} <$ 350 GeV. The distribution for the POWHEG formalism (solid blue line) is plotted together with the distribution for the Herwig++ parton shower (dashed red line). The data are from ref. [83] and the lower frame is as described in figure 5

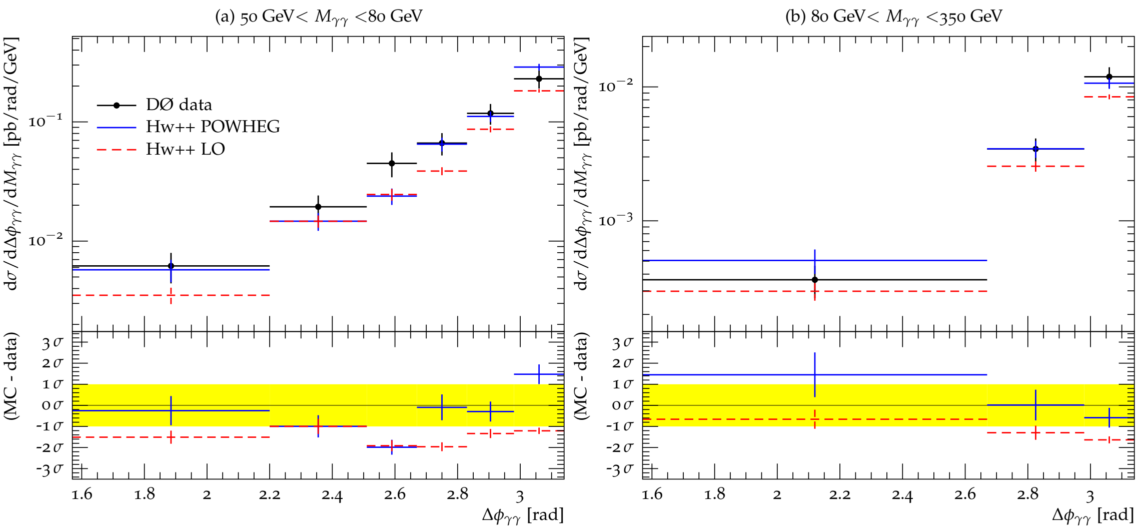


**Figure 7**. Azimuthal angle between the photons for (a) 50 GeV $< M_{\gamma\gamma} <$ 80 GeV and (b) 80 GeV $< M_{\gamma\gamma} <$ 350 GeV. The solid blue line shows the result for the Herwig++ shower with POWHEG corrections, while the red dashed line gives the result from the Herwig++ parton shower. The data are from ref. [83] and the lower frame is as described in figure 5

and the NLO variation is not much smaller than the LO one because there is only a small scale uncertainty in the LO $q\bar{q} \to \gamma\gamma$ component. Most of the variation is in the $\gamma$jet contribution and its uncertainty is essentially the same at NLO in our approach.

JHEP02(2012)130

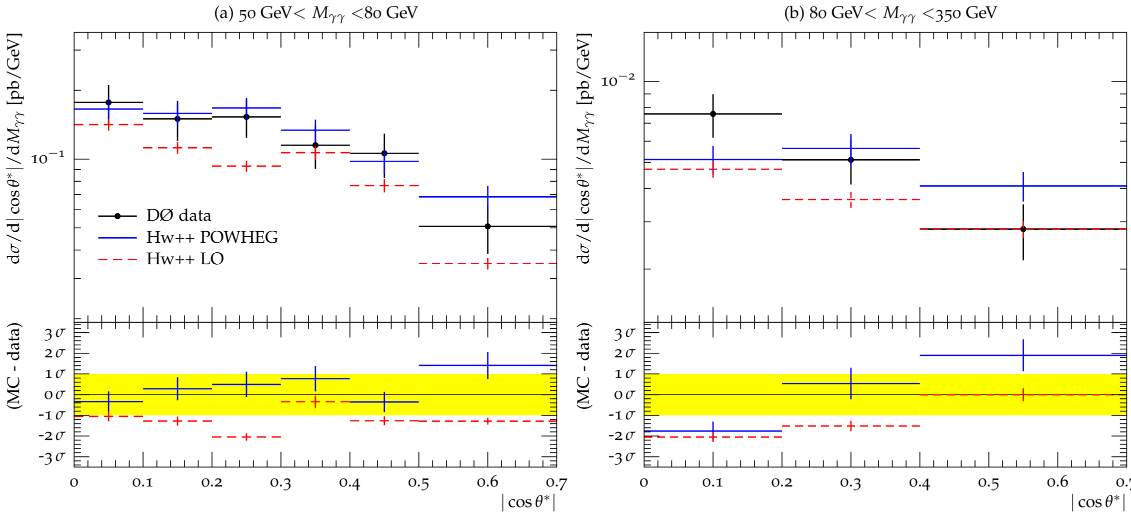


**Figure 8**. Polar scattering angle between the photons for two ranges of $M_{\gamma\gamma}$: 50 GeV $< M_{\gamma\gamma} <$ 80 GeV (a) and 80 GeV $< M_{\gamma\gamma} <$ 350 GeV (b). The solid blue line describes the Herwig++ result with POWHEG corrections, the dashed red line does not include matrix element corrections. The data are from ref. [83] and the lower frame is as described in figure 5.

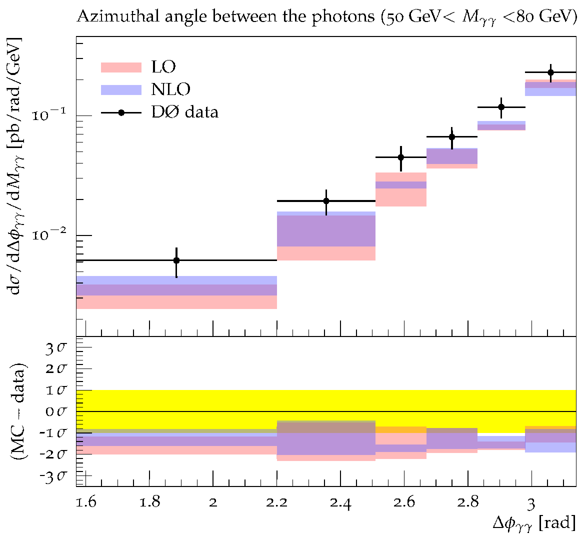


**Figure 9**. In the present figure we show scale variation for the azimuthal angle between the photons for 50 GeV $< M_{\gamma\gamma} <$ 80 GeV.

## 6 Conclusion

In the present work the POWHEG NLO matching scheme has been extended and applied to $\gamma\gamma$-production in hadron collisions. The QED singularities are not treated by including fragmentation functions but rather by simulating the LO cross section for the corresponding process and then showering it. The simulation contains a full treatment of the truncated shower which is needed to correctly generate radiation with transverse momentum that is smaller than the one of the hardest emission.

The implementation of the process was tested by comparing the results with the fixed-order DIPHOX program which is in good agreement with the results of our approach for observables which are not sensitive to multiple QCD radiation.

We find that without a correction to describe the hard QCD radiation there is a deficit of radiation in the simulation. The POWHEG approach overcomes this problem and provides a good description of the data of refs. [83, 84]. A remarkably good description is obtained for infrared sensitive observables, like the transverse momentum of the $\gamma\gamma$-pair at low $p_\perp^{\gamma\gamma}$, which demonstrates the resummation of logarithmic enhancement provided by the Herwig++ parton shower.

This is the first NLO simulation of a process involving photons and provides an important new tool for the study of promt photon production. The simulation will be made available in a forthcoming version of the Herwig++ simulation package.

## References


[1] A. Buckley, J. Butterworth, S. Gieseke, D. Grellscheid, S. Hoche, et al., *General-purpose event generators for LHC physics*, Phys. Rept. **504** (2011) 145 [arXiv:1101.2599] [INSPIRE].

[2] T. Sjöstrand and M. Bengtsson, *The Lund Monte Carlo for jet fragmentation and $e^+e^-$ physics. JETSET version 6.3: an update*, Comput. Phys. Commun. **43** (1987) 367 [INSPIRE].

[3] M. Bengtsson and T. Sjöstrand, *Parton showers in leptoproduction events*, Z. Phys. **C 37** (1988) 465 [INSPIRE].

[4] E. Norrbin and T. Sjöstrand, *QCD radiation off heavy particles*, Nucl. Phys. **B 603** (2001) 297 [hep-ph/0010012] [INSPIRE].

[5] G. Miu and T. Sjöstrand, *W production in an improved parton shower approach*, Phys. Lett. **B 449** (1999) 313 [hep-ph/9812455] [INSPIRE].

[6] G. Corcella, I. Knowles, G. Marchesini, S. Moretti, K. Odagiri, et al., *HERWIG 6: an event generator for hadron emission reactions with interfering gluons (including supersymmetric processes)*, JHEP **01** (2001) 010 [hep-ph/0011363] [INSPIRE].

[7] G. Corcella, I. Knowles, G. Marchesini, S. Moretti, K. Odagiri, et al., *HERWIG 6.5 release note*, hep-ph/0210213 [INSPIRE].

[8] M.H. Seymour, *Photon radiation in final state parton showering*, Z. Phys. **C 56** (1992) 161 [INSPIRE].

[9] M.H. Seymour, *Matrix element corrections to parton shower simulation of deep inelastic scattering*, talk contributed to the *27th International Conference on High Energy Physics (ICHEP)*, Glasgow Scotland, 20-27 July 1994.

[10] G. Corcella and M. Seymour, *Matrix element corrections to parton shower simulations of heavy quark decay*, Phys. Lett. **B 442** (1998) 417 [hep-ph/9809451] [INSPIRE].

[11] G. Corcella and M.H. Seymour, *Initial state radiation in simulations of vector boson production at hadron colliders*, Nucl. Phys. **B 565** (2000) 227 [hep-ph/9908388] [INSPIRE].

[12] M.H. Seymour, *Matrix element corrections to parton shower algorithms*, Comput. Phys. Commun. **90** (1995) 95 [hep-ph/9410414] [INSPIRE].

[13] M.H. Seymour, *A simple prescription for first order corrections to quark scattering and annihilation processes*, Nucl. Phys. **B 436** (1995) 443 [hep-ph/9410244] [INSPIRE].

[14] S. Gieseke, A. Ribon, M.H. Seymour, P. Stephens and B. Webber, *HERWIG++ 1.0: an event generator for $e^+e^-$ annihilation*, JHEP **02** (2004) 005 [hep-ph/0311208] [INSPIRE].

[15] S. Gieseke, *The new Monte Carlo event generator HERWIG++*, hep-ph/0408034 [INSPIRE].

[16] K. Hamilton and P. Richardson, *A simulation of QCD radiation in top quark decays*, JHEP **02** (2007) 069 [hep-ph/0612236] [INSPIRE].

[17] S. Gieseke, D. Grellscheid, K. Hamilton, A. Ribon, P. Richardson, et al., *HERWIG++ 2.0 release note*, hep-ph/0609306 [INSPIRE].

[18] M. Bahr, S. Gieseke, M. Gigg, D. Grellscheid, K. Hamilton, et al., *HERWIG++ 2.2 release note*, arXiv:0804.3053 [INSPIRE].

[19] S. Gieseke, D. Grellscheid, K. Hamilton, A. Papaefstathiou, S. Platzer, et al., *HERWIG++ 2.5 release note*, arXiv:1102.1672 [INSPIRE].

[20] S. Catani, F. Krauss, R. Kuhn and B. Webber, *QCD matrix elements + parton showers*, JHEP **11** (2001) 063 [hep-ph/0109231] [INSPIRE].

[21] F. Krauss, *Matrix elements and parton showers in hadronic interactions*, JHEP **08** (2002) 015 [hep-ph/0205283] [INSPIRE].

[22] L. Lönnblad, *Correcting the color dipole cascade model with fixed order matrix elements*, JHEP **05** (2002) 046 [hep-ph/0112284] [INSPIRE].

[23] A. Schalicke and F. Krauss, *Implementing the ME+PS merging algorithm*, JHEP **07** (2005) 018 [hep-ph/0503281] [INSPIRE].

[24] F. Krauss, A. Schalicke and G. Soff, *APACIC++ 2.0: a parton cascade in C++*, Comput. Phys. Commun. **174** (2006) 876 [hep-ph/0503087] [INSPIRE].

[25] N. Lavesson and L. Lönnblad, *W+jets matrix elements and the dipole cascade*, JHEP **07** (2005) 054 [hep-ph/0503293] [INSPIRE].

[26] S. Mrenna and P. Richardson, *Matching matrix elements and parton showers with HERWIG and PYTHIA*, JHEP **05** (2004) 040 [hep-ph/0312274] [INSPIRE].

[27] M.L. Mangano, M. Moretti, F. Piccinini, R. Pittau and A.D. Polosa, *ALPGEN, a generator for hard multiparton processes in hadronic collisions*, JHEP **07** (2003) 001 [hep-ph/0206293] [INSPIRE].

[28] J. Alwall, S. Hoche, F. Krauss, N. Lavesson, L. Lönnblad, et al., *Comparative study of various algorithms for the merging of parton showers and matrix elements in hadronic collisions*, Eur. Phys. J. **C 53** (2008) 473 [arXiv:0706.2569] [INSPIRE].

[29] S. Hoeche, F. Krauss, S. Schumann and F. Siegert, *QCD matrix elements and truncated showers*, JHEP **05** (2009) 053 [arXiv:0903.1219] [INSPIRE].

[30] K. Hamilton, P. Richardson and J. Tully, *A modified CKKW matrix element merging approach to angular-ordered parton showers*, JHEP **11** (2009) 038 [arXiv:0905.3072] [INSPIRE].

[31] S. Frixione and B.R. Webber, *Matching NLO QCD computations and parton shower simulations*, JHEP **06** (2002) 029 [hep-ph/0204244] [INSPIRE].



JHEP02(2012)130

[32] S. Frixione, F. Stoeckli, P. Torrielli, B.R. Webber and C.D. White, *The MCaNLO 4.0 event generator*, arXiv:1010.0819 [INSPIRE].

[33] S. Frixione, E. Laenen, P. Motylinski and B.R. Webber, *Single-top production in MC@NLO*, *JHEP* **03** (2006) 092 [hep-ph/0512250] [INSPIRE].

[34] S. Frixione, E. Laenen, P. Motylinski and B.R. Webber, *Angular correlations of lepton pairs from vector boson and top quark decays in Monte Carlo simulations*, *JHEP* **04** (2007) 081 [hep-ph/0702198] [INSPIRE].

[35] S. Frixione, E. Laenen, P. Motylinski, B.R. Webber and C.D. White, *Single-top hadroproduction in association with a W boson*, *JHEP* **07** (2008) 029 [arXiv:0805.3067] [INSPIRE].

[36] O. Latunde-Dada, *HERWIG Monte Carlo at next-to-leading order for $e^+e^-$ annihilation and lepton pair production*, *JHEP* **11** (2007) 040 [arXiv:0708.4390] [INSPIRE].

[37] O. Latunde-Dada, *MC and NLO for the hadronic decay of Higgs bosons in associated production with vector bosons*, *JHEP* **05** (2009) 112 [arXiv:0903.4135] [INSPIRE].

[38] A. Papaefstathiou and O. Latunde-Dada, *NLO production of W ' bosons at hadron colliders using the MC@NLO and POWHEG methods*, *JHEP* **07** (2009) 044 [arXiv:0901.3685] [INSPIRE].

[39] P. Torrielli and S. Frixione, *Matching NLO QCD computations with PYTHIA using MC@NLO*, *JHEP* **04** (2010) 110 [arXiv:1002.4293] [INSPIRE].

[40] S. Frixione, F. Stoeckli, P. Torrielli and B.R. Webber, *NLO QCD corrections in HERWIG++ with MC@NLO*, *JHEP* **01** (2011) 053 [arXiv:1010.0568] [INSPIRE].

[41] P. Nason, *A new method for combining NLO QCD with shower Monte Carlo algorithms*, *JHEP* **11** (2004) 040 [hep-ph/0409146] [INSPIRE].

[42] S. Frixione, P. Nason and C. Oleari, *Matching NLO QCD computations with parton shower simulations: the POWHEG method*, *JHEP* **11** (2007) 070 [arXiv:0709.2092] [INSPIRE].

[43] P. Nason and G. Ridolfi, *A positive-weight next-to-leading-order Monte Carlo for Z pair hadroproduction*, *JHEP* **08** (2006) 077 [hep-ph/0606275] [INSPIRE].

[44] S. Frixione, P. Nason and G. Ridolfi, *A positive-weight next-to-leading-order Monte Carlo for heavy flavour hadroproduction*, *JHEP* **09** (2007) 126 [arXiv:0707.3088] [INSPIRE].

[45] O. Latunde-Dada, S. Gieseke and B. Webber, *A positive-weight next-to-leading-order Monte Carlo for $e^+e^-$ annihilation to hadrons*, *JHEP* **02** (2007) 051 [hep-ph/0612281] [INSPIRE].

[46] S. Alioli, P. Nason, C. Oleari and E. Re, *NLO vector-boson production matched with shower in POWHEG*, *JHEP* **07** (2008) 060 [arXiv:0805.4802] [INSPIRE].

[47] K. Hamilton, P. Richardson and J. Tully, *A positive-weight next-to-leading order Monte Carlo simulation of Drell-Yan vector boson production*, *JHEP* **10** (2008) 015 [arXiv:0806.0290] [INSPIRE].

[48] S. Alioli, P. Nason, C. Oleari and E. Re, *NLO Higgs boson production via gluon fusion matched with shower in POWHEG*, *JHEP* **04** (2009) 002 [arXiv:0812.0578] [INSPIRE].

[49] K. Hamilton, P. Richardson and J. Tully, *A positive-weight next-to-leading order Monte Carlo simulation for Higgs boson production*, *JHEP* **04** (2009) 116 [arXiv:0903.4345] [INSPIRE].


JHEP02(2012)130

[50] S. Alioli, P. Nason, C. Oleari and E. Re, *NLO single-top production matched with shower in POWHEG: s- and t-channel contributions*, *JHEP* **09** (2009) 111 [*Erratum ibid.* **1002** (2010) 011] [arXiv:0907.4076] [INSPIRE].

[51] S. Hoche, F. Krauss, M. Schonherr and F. Siegert, *Automating the POWHEG method in SHERPA*, *JHEP* **04** (2011) 024 [arXiv:1008.5399] [INSPIRE].

[52] S. Alioli, P. Nason, C. Oleari and E. Re, *A general framework for implementing NLO calculations in shower Monte Carlo programs: the POWHEG BOX*, *JHEP* **06** (2010) 043 [arXiv:1002.2581] [INSPIRE].

[53] P. Nason and C. Oleari, *NLO Higgs boson production via vector-boson fusion matched with shower in POWHEG*, *JHEP* **02** (2010) 037 [arXiv:0911.5299] [INSPIRE].

[54] E. Re, *Single-top production with the POWHEG method*, *PoS* **DIS2010** (2010) 172 [arXiv:1007.0498] [INSPIRE].

[55] E. Re, *Single-top Wt-channel production matched with parton showers using the POWHEG method*, *Eur. Phys. J.* **C 71** (2011) 1547 [arXiv:1009.2450] [INSPIRE].

[56] S. Alioli, P. Nason, C. Oleari and E. Re, *Vector boson plus one jet production in POWHEG*, *JHEP* **01** (2011) 095 [arXiv:1009.5594] [INSPIRE].

[57] S. Alioli, K. Hamilton, P. Nason, C. Oleari and E. Re, *Jet pair production in POWHEG*, *JHEP* **04** (2011) 081 [arXiv:1012.3380] [INSPIRE].

[58] C. Oleari, *The POWHEG-BOX*, *Nucl. Phys. Proc. Suppl.* **205-206** (2010) 36 [arXiv:1007.3893] [INSPIRE].

[59] K. Hamilton, *A positive-weight next-to-leading order simulation of weak boson pair production*, *JHEP* **01** (2011) 009 [arXiv:1009.5391] [INSPIRE].

[60] C. Oleari and L. Reina, *$W^{+-}b\bar{b}$ production in POWHEG*, *JHEP* **08** (2011) 061 [*Erratum ibid.* **1111** (2011) 040] [arXiv:1105.4488] [INSPIRE].

[61] A. Kardos, C. Papadopoulos and Z. Trócsányi, *Top quark pair production in association with a jet with NLO parton showering*, *Phys. Lett.* **B 705** (2011) 76 [arXiv:1101.2672] [INSPIRE].

[62] T. Melia, P. Nason, R. Rontsch and G. Zanderighi, *$W^+W^-$ plus dijet production in the POWHEGBOX*, *Eur. Phys. J.* **C 71** (2011) 1670 [arXiv:1102.4846] [INSPIRE].

[63] N. Lavesson and L. Lönnblad, *Extending CKKW-merging to one-loop matrix elements*, *JHEP* **12** (2008) 070 [arXiv:0811.2912] [INSPIRE].

[64] K. Hamilton and P. Nason, *Improving NLO-parton shower matched simulations with higher order matrix elements*, *JHEP* **06** (2010) 039 [arXiv:1004.1764] [INSPIRE].

[65] S. Hoche, F. Krauss, M. Schonherr and F. Siegert, *NLO matrix elements and truncated showers*, *JHEP* **08** (2011) 123 [arXiv:1009.1127] [INSPIRE].

[66] H. Baer, J. Ohnemus and J. Owens, *A next-to-leading logarithm calculation of direct photon production*, *Phys. Rev.* **D 42** (1990) 61 [INSPIRE].

[67] P. Aurenche, R. Baier and M. Fontannaz, *Prompt photon production at colliders*, *Phys. Rev.* **D 42** (1990) 1440 [INSPIRE].

[68] E. Glover and A. Morgan, *Measuring the photon fragmentation function at LEP*, *Z. Phys.* **C 62** (1994) 311 [INSPIRE].


JHEP02(2012)130

[69] S. Frixione, *Isolated photons in perturbative QCD*, Phys. Lett. **B 429** (1998) 369 [hep-ph/9801442] [INSPIRE].

[70] S. Hoeche, S. Schumann and F. Siegert, *Hard photon production and matrix-element parton-shower merging*, Phys. Rev. **D 81** (2010) 034026 [arXiv:0912.3501] [INSPIRE].

[71] D0 collaboration, V. Abazov et al., *Search for resonant diphoton production with the D0 detector*, Phys. Rev. Lett. **102** (2009) 231801 [arXiv:0901.1887] [INSPIRE].

[72] The ATLAS collaboration, G. Aad et al., *Expected performance of the ATLAS experiment - Detector, trigger and physics*, arXiv:0901.0512 [INSPIRE].

[73] CMS collaboration, G. Bayatian et al., *CMS technical design report, volume II: physics performance*, J. Phys. **G 34** (2007) 995 [INSPIRE].

[74] S. Mrenna and J.D. Wells, *Detecting a light Higgs boson at the Fermilab Tevatron through enhanced decays to photon pairs*, Phys. Rev. **D 63** (2001) 015006 [hep-ph/0001226] [INSPIRE].

[75] T. Han, J.D. Lykken and R.-J. Zhang, *On Kaluza-Klein states from large extra dimensions*, Phys. Rev. **D 59** (1999) 105006 [hep-ph/9811350] [INSPIRE].

[76] G. Giudice and R. Rattazzi, *Theories with gauge mediated supersymmetry breaking*, Phys. Rept. **322** (1999) 419 [hep-ph/9801271] [INSPIRE].

[77] WA70 collaboration, E. Bonvin et al., *Intrinsic transverse momentum in the $\pi^- p \to \gamma\gamma X$ reaction at 280 GeV/c*, Phys. Lett. **B 236** (1990) 523 [INSPIRE].

[78] WA70 collaboration, E. Bonvin et al., *Double prompt photon production at high transverse momentum by $\pi^-$ on protons at 280 GeV/c*, Z. Phys. **C 41** (1989) 591 [INSPIRE].

[79] E706 collaboration, M. Begel, *Photons and diphotons from E706*, Nucl. Phys. Proc. Suppl. **79** (1999) 244 [INSPIRE].

[80] UA1 collaboration, C. Albajar et al., *Direct photon production at the CERN proton - anti-Proton collider*, Phys. Lett. **B 209** (1988) 385 [INSPIRE].

[81] UA2 collaboration, J. Alitti et al., *A measurement of single and double prompt photon production at the CERN $\bar{p}p$ collider*, Phys. Lett. **B 288** (1992) 386 [INSPIRE].

[82] CDF collaboration, F. Abe et al., *Measurement of the cross-section for production of two isolated prompt photons in $\bar{p}p$ collisions at $\sqrt{s} = 1.8$ TeV*, Phys. Rev. Lett. **70** (1993) 2232 [INSPIRE].

[83] CDF collaboration, D. Acosta et al., *Measurement of the cross section for prompt diphoton production in $p\bar{p}$ collisions at $\sqrt{s} = 1.96$ TeV*, Phys. Rev. Lett. **95** (2005) 022003 [hep-ex/0412050] [INSPIRE].

[84] The D0 collaboration, V. Abazov et al., *Measurement of direct photon pair production cross sections in $p\bar{p}$ collisions at $\sqrt{s} = 1.96$ TeV*, Phys. Lett. **B 690** (2010) 108 [arXiv:1002.4917] [INSPIRE].

[85] E.L. Berger, E. Braaten and R. Field, *Large $p_T$ production of single and double photons in proton proton and pion-proton collisions*, Nucl. Phys. **B 239** (1984) 52 [INSPIRE].

[86] C. Llewellyn Smith, *QCD predictions for processes involving real photons*, Phys. Lett. **B 79** (1978) 83 [INSPIRE].

[87] P. Aurenche, R. Baier, M. Fontannaz and D. Schiff, *Prompt photon production at large $p_T$ scheme invariant QCD predictions and comparison with experiment*, *Nucl. Phys.* **B 297** (1988) 661 [INSPIRE].

[88] L. Gordon and W. Vogelsang, *Polarized and unpolarized isolated prompt photon production beyond the leading order*, *Phys. Rev.* **D 50** (1994) 1901 [INSPIRE].

[89] P. Aurenche, A. Douiri, R. Baier, M. Fontannaz and D. Schiff, *Large $p_T$ double photon production in hadronic collisions: beyond leading logarithm QCD calculation*, *Z. Phys.* **C 29** (1985) 459 [INSPIRE].

[90] B. Bailey, J. Owens and J. Ohnemus, *An order $\alpha_s$ Monte Carlo calculation of hadronic double photon production*, *Phys. Rev.* **D 46** (1992) 2018 [INSPIRE].

[91] V. Del Duca, F. Maltoni, Z. Nagy and Z. Trócsányi, *QCD radiative corrections to prompt diphoton production in association with a jet at hadron colliders*, *JHEP* **04** (2003) 059 [hep-ph/0303012] [INSPIRE].

[92] S. Catani, M. Fontannaz, J. Guillet and E. Pilon, *Cross-section of isolated prompt photons in hadron hadron collisions*, *JHEP* **05** (2002) 028 [hep-ph/0204023] [INSPIRE].

[93] T. Binoth, J. Guillet, E. Pilon and M. Werlen, *A full next-to-leading order study of direct photon pair production in hadronic collisions*, *Eur. Phys. J.* **C 16** (2000) 311 [hep-ph/9911340] [INSPIRE].

[94] S. Catani and M. Seymour, *A general algorithm for calculating jet cross-sections in NLO QCD*, *Nucl. Phys.* **B 485** (1997) 291 [*Erratum ibid.* **B 510** (1998) 503-504] [hep-ph/9605323] [INSPIRE].

[95] S. Frixione, Z. Kunszt and A. Signer, *Three jet cross-sections to next-to-leading order*, *Nucl. Phys.* **B 467** (1996) 399 [hep-ph/9512328] [INSPIRE].

[96] M. Bahr, S. Gieseke, M. Gigg, D. Grellscheid, K. Hamilton, et al., *HERWIG++ physics and manual*, *Eur. Phys. J.* **C 58** (2008) 639 [arXiv:0803.0883] [INSPIRE].

[97] L. Lönnblad, *ThePEG, PYTHIA7, HERWIG++ and Ariadne*, *Nucl. Instrum. Meth.* **A 559** (2006) 246 [INSPIRE].

[98] T. Sjöstrand, S. Mrenna and P.Z. Skands, *PYTHIA 6.4 physics and manual*, *JHEP* **05** (2006) 026 [hep-ph/0603175] [INSPIRE].

[99] W.-K. Tung, *New generation of parton distributions with uncertainties from global QCD analysis*, *Acta Phys. Polon.* **B 33** (2002) 2933 [hep-ph/0206114] [INSPIRE].

[100] C. Balázs, E.L. Berger, S. Mrenna and C. Yuan, *Photon pair production with soft gluon resummation in hadronic interactions*, *Phys. Rev.* **D 57** (1998) 6934 [hep-ph/9712471] [INSPIRE].

[101] C. Balázs, E.L. Berger, P.M. Nadolsky and C.-P. Yuan, *Calculation of prompt diphoton production cross-sections at Tevatron and LHC energies*, *Phys. Rev.* **D 76** (2007) 013009 [arXiv:0704.0001] [INSPIRE].

[102] P.M. Nadolsky, C. Balázs, E.L. Berger and C.-P. Yuan, *Gluon-gluon contributions to the production of continuum diphoton pairs at hadron colliders*, *Phys. Rev.* **D 76** (2007) 013008 [hep-ph/0702003] [INSPIRE].

[103] P.M. Nadolsky and C. Schmidt, *Diphoton production in gluon fusion at small transverse momentum*, *Phys. Lett.* **B 558** (2003) 63 [hep-ph/0211398] [INSPIRE].

[104] C. Balázs, P.M. Nadolsky, C. Schmidt and C. Yuan, *Diphoton background to Higgs boson production at the LHC with soft gluon effects*, Phys. Lett. **B 489** (2000) 157 [hep-ph/9905551] [INSPIRE].

[105] A. Buckley, J. Butterworth, L. Lönnblad, H. Hoeth, J. Monk, et al., *Rivet user manual*, arXiv:1003.0694 [INSPIRE].

[106] C. Balázs, E.L. Berger, P.M. Nadolsky and C.-P. Yuan, *All-orders resummation for diphoton production at hadron colliders*, Phys. Lett. **B 637** (2006) 235 [hep-ph/0603037] [INSPIRE].